MULTIVARIABLE H_2 AND H_∞ CONTROL FOR WIND ENERGY CONVERSION SYSTEM - A COMPARISON

Ronilson Rocha
Federal University of Ouro Preto
EM/DECAT
Campus Morro do Cruzeiro, 35400-000, Ouro Preto, MG, Brazil
rocha@em.ufop.br

Luiz Siqueira Martins Filho
Federal University of Minas Gerais
ICEB/DECOM
Campus Morro do Cruzeiro, 35400-000, Ouro Preto, MG, Brazil
luizm@iceb.ufop.br

Marcos V. Bortolus
Federal University of Minas Gerais
DEMEC
Campus Pampulha, 30161-970, Belo Horizonte, MG, Brazil
borta@demec.ufmg.br

Abstract. *The wind energy is a renewable and pollution-free source. The aerodynamic behavior of a Wind Energy Conversion System (WECS) is nonlinear, highly dependent of wind speed and subjected to cyclical variations, whose introduce periodic disturbances in the system. In this context, the controller design for a WECS consists in an interesting problem for control theory, since its qualities is determined by its capacity to deal with unmodelled dynamics, exogenous stochastic signal and periodic disturbances. Considering that WECS objectives can be easily specified in terms of maximum allowable gain in the disturbance-to-output transfer functions, H_2 and H_∞ methodologies consist in good options to control design for WECS. The H_2 philosophy is particularly appropriate in situations where disturbance rejection and noise suppression are important, while H_∞ is usually preferred when the robustness to plant uncertainties is the dominant issue. Both methodologies offer the capability of stabilizing the plant disturbance and a trade-off between performance and control effort, combining several specifications such as disturbance attenuation, asymptotic tracking, bandwidth limitation and robust stability. In this paper, multivariable feedback controllers are designed for a WECS applying H_2 and H_∞ methodologies. The performance of both designs will be analyzed and compared using computer simulations.*

Keywords. control theory, H_2 control, H_∞ control

1. Introduction

Wind Energy Conversion System (WECS) has attracted a growing interest in the last years since it can offer, from a renewable and pollution-free source, a significant contribution to support electric energy demand. Its basic configuration is a wind turbine (WT) coupled to an electric generator, directly or through gear-box. In spite of its simplicity, this system can represent an interesting problem in viewpoint of control theory. The aerodynamic characteristic of a WT is nonlinear and highly dependent of wind speed, which is an energy source with stochastic behavior and subjected to sudden variations, such as impulses and steps. Tower shadow, wind shear, yaw misalignment and shaft tilt cause cyclical variations on WT loading, introducing a periodical ripple torque on WECS (Freris, 1990).

Simplest WECS configuration uses a stall regulated WT, where control speed is realized by stall effect through of adjusts on the electric load connected to generator (Novak *et al.*, 1995). In any WT configurations, it is possible to vary the pitch angle of turbine blades aiming to regulate its aerodynamic efficiency and, consequently, its speed and power (Wasynczuk *et al.*, 1981). Although the yaw misalignment and shaft tilt can be used to control WT speed and power, these methods are rarely used (Freris, 1990). Since an exact WECS model is a complex problem due to difficult characterization of physical phenomenon by means of experimental investigation, the control system has to deal with several system uncertainties such as parameter variations, nonlinearities, noise or unmodeled dynamics. In this context, a WECS can be considered a multivariable system subject to unmodelled dynamics and non periodic disturbances, which controller quality is measured by its stochastic properties and its capacity to establish a trade-off between to reduce mechanical stress and to increase the energy captured from wind.

The basic control requirements for a WECS are to regulate WT speed and power aiming to reduce detrimental

dynamic loads and to maximize efficiency on energy conversion, shaping system dynamics to satisfy the performance and stability specifications under varying wind conditions(Leithead *et al.*, 1991). Another important control objective is to reduce the influence of wind fluctuation and ripple torque on WECS at any rotation speed, whose introduce unavoidable vibrations along the drive-line with detrimental effects on WECS, resulting in large power fluctuations available to costumers and contributing greatly to the fatigue of various mechanical components (Dessaint *et al.*, 1986). In many WECS, WT speed must be controlled to restrict speed variations since the generator is directly connected to fixed-frequency electrical load. However, advances on Power Electronics and Control Systems technologies have became interesting the use of variable-speed WECS, which offers important advantages, such as the increase of energy captured from the wind, reduction of fatigue damage on rotor blades and drive train, reduction of aerodynamic acoustic noise level and operational flexibility (Novak *et al.*, 1995; Manwell *et al.*, 1991).

Although the classical methods are traditionally utilized to design controllers for WECS (Leithead *et al.*, 1991; Dessaint *et al.*, 1986; Lefevbre and Dubé, 1988), they do not offer a completely satisfactory solution, since they do not assure the robustness for both stability and performance, resulting in controllers that are not able to provide a good tolerance to WECS uncertainties. Considering that WECS objectives can be easily specified in terms of maximum allowable gain in the disturbance-to-output transfer functions, H_2 and H_∞ methodologies consist in good options to control design for WECS (Maciejowski, 1989). The H_2 philosophy is particularly appropriate in situations where disturbance rejection and noise suppression are important, while H_∞ is usually preferred when the robustness to plant uncertainties is the dominant issue. Both methodologies offer the capability of stabilizing the plant disturbance and a trade-off between performance and control effort, combining several specifications such as disturbance attenuation, asymptotic tracking, bandwidth limitation and robust stability.

In this work, H_2 and H_∞ methodologies are utilized on feedback controller design for a multivariable WECS. The section 2. presents a linearized model for WECS, which is augmented aiming to weight control objetives in the section 3.. H_2 methodology is presented in the section 4., while section 5. describes H_∞ controller design. For both resulting controllers, the dynamic response of close-loop system is simulated using a nonlinear model of a WT presented in (Wasynczuk *et al.*, 1981). From simulation results, both resulting controllers are analized and compared on the section 6..

2. WECS Nominal Model

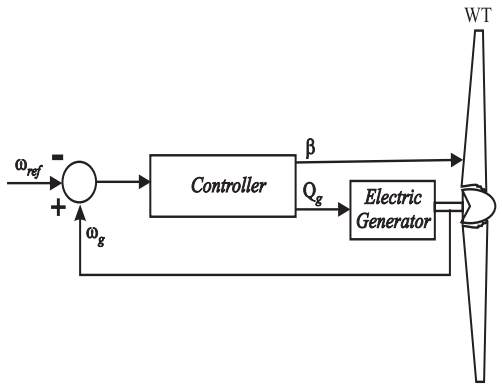

Figure 1. Speed feedback control system structure

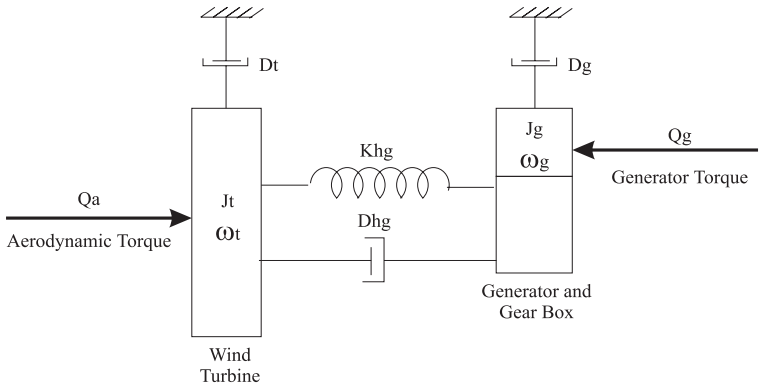

Figure 2. WECS Model

The control structure considered for this modelling is shown in the figure 1. The schematic diagram in the figure 2 shows the basic configuration of a WECS, constituted by a WT, electric generator and mechanical coupling. The aerodynamic behavior of the wind turbine is nonlinear, dependent of wind speed and it may change over time due to contamination of blade surfaces. In general, dimensionless coeficients that define the WT ability to convert kinetic energy of moving air into mechanical power C_p or torque C_q are used to evaluate the aerodynamic torque Q_a of a WT. Both coefficients C_p e C_q are nonlinear functions of pitch angle β, yaw angle θ and a parameter known as tip-speed ratio λ defined as:

$$\lambda = \frac{R\omega_t}{V} \tag{1}$$

where R= turbine radius, ω_t= turbine speed and V= wind speed. Admitting that WT is always aligned with wind direction, i.e. $\theta = 0^o$, the aerodynamic torque Q_a is given by (Freris, 1990; Novak *et al.*, 1995; Wasynczuk *et al.*, 1981):

$$Q_a = \frac{1}{2}\rho AR\frac{C_p(\lambda,\beta)}{\lambda}V^2 = \frac{1}{2}\rho ARC_q(\lambda,\beta)V^2 \tag{2}$$

where ρ= air density and A= rotor area.

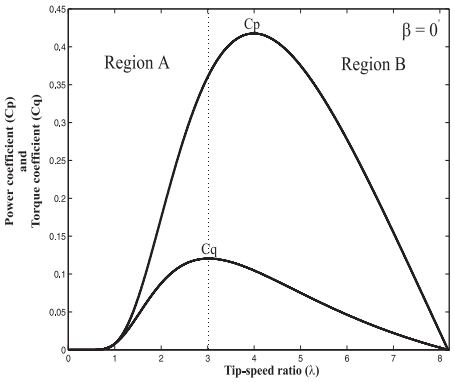

Figure 3. Aerodynamic Characteristics of a WT

The C_p and C_q characteristics for $\beta = 0^o$ are shown in the figure 3. From curve $C_q \times \lambda$, it is possible to note two distinct regions in the WT operation: the unstable stall region (A), characterized by a positive slope, where occurs a suddenly and significantly drops on aerodynamic torque, and the stable operation region (B), characterized by a negative slope, which corresponding to normal operation of WT where the aerodynamic torque Q_a can be linearized for control design without degeneration of the results as (Novak *et al.*, 1995; Rocha and Martins Filho, 2003):

$$\dot{Q}_a = \alpha\dot{V} + \gamma\dot{\omega}_t + \kappa\dot{\beta} \tag{3}$$

where α is a scaling factor for torque disturbance due to wind variations $\dot{V}$, γ denotes the speed-feedback coefficient from drive-train and κ represents the pitch control gain. In steady state, $\dot{V}$ is the wind fluctuation, which can be assumed as white noise with zero mean (Wasynczuk *et al.*, 1981). Since it is desirable to operate at maximum C_p, the aerodynamic torque linearization can be performed in the corresponding λ_{opt}, which is always situated in normal operation region. Considering $\bar{V}$ as the nominal wind speed on WECS location, the coefficients α, γ and κ can be easily computed from wind turbine data as:

$$\alpha = \left.\frac{\partial Q_a}{\partial V}\right|_{\lambda_{opt}} = \frac{3}{2}\rho AR\frac{C_{p_{opt}}}{\lambda_{opt}}\bar{V} \tag{4}$$

$$\gamma = \left.\frac{\partial Q_a}{\partial \omega_t}\right|_{\lambda_{opt}} = -\frac{1}{2}\rho AR^2\frac{C_{p_{opt}}}{\lambda_{opt}^2}\bar{V} \tag{5}$$

$$\kappa = \left.\frac{\partial Q_a}{\partial \beta}\right|_{\lambda_{opt}} = \frac{1}{2}\rho AR\bar{V}^2\left.\frac{\partial C_q}{\partial \beta}\right|_{\lambda_{opt}} \tag{6}$$

The turbine speed ω_t is obtained from drive-train modelling. Although a real mechanical drive train has rigid disks, flexible shaft elements with distributed mass and stiffness, an approximated to 2-mass model is enough to fit the dynamic behavior of the WT drive train. Admitting an ideal gear-box and reducing all quantities to primary side,

the mechanical couple can be described using classical rotational dynamic (Leith and Leithead, 1997):

$$J_t\dot{\omega_t} + D_t\omega_t = Q_a - Q_m - D_{hg}\left(\omega_t - \omega_g\right) \tag{7}$$

$$J_g\dot{\omega_g} + D_g\omega_g = D_{hg}\left(\omega_t - \omega_g\right) + Q_m - Q_g \tag{8}$$

$$Q_m = K_{hg}\int\left(\omega_t - \omega_g\right)dt \tag{9}$$

where ω_g= generator speed, J_t= turbine inertia, J_g= generator inertia, D_t= turbine damping, D_g= generator damping, D_{hg}= shaft damping, K_{hg}= shaft stiffness, Q_a= aerodynamic torque, Q_g= generator torque and Q_m= shaft torque.

The structural dynamics can be considered as unmodelled uncertainties. Since electrical generator is the interface between mechanical energy and electricity, the generator torque Q_g represents the electric load connected to generator seen by mechanical system. Considering that electric load is adjustable and virtually independent of WECS dynamics (Novak *et al.*, 1995), the generator torque Q_g consists in one of control inputs. Another control input is the pitch angle β. The exogeneous inputs on WECS are the speed reference ω_{sp} and wind fluctuation $\dot{V}$. Due to practical constraint relatives to assembler, cost and maintainance of sensor for shaft torque and turbine speed measurements, this work considers the generator speed ω_g as the only measured output y.

3. Weighting Functions

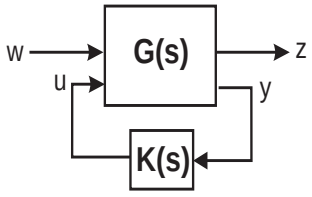

Figure 4. Generalized system

A H_2 or H_∞ optimal feedback control problem consists in to find a controller $\mathbf{K}$ for a generalized system $\mathbf{G}(s)$ shown in the figure 4 using optimization problems involving respective norms. Aiming to obtain satisfatory trade-off between stability, performance and robustness requirements, the nominal model have to be manipulated using weighting functions, resulting in a generalized system $\mathbf{G}(s)$ given by:

$$\mathbf{G}(s) = \begin{cases} \dot{\mathbf{x}} = \mathbf{A}\mathbf{x} + \mathbf{B_1}\mathbf{w} + \mathbf{B_2}\mathbf{u} \\ \mathbf{z} = \mathbf{C_1}\mathbf{x} + \mathbf{D_{11}}\mathbf{w} + \mathbf{D_{12}}\mathbf{u} \\ \mathbf{y} = \mathbf{C_2}\mathbf{x} + \mathbf{D_{21}}\mathbf{w} + \mathbf{D_{22}}\mathbf{u} \end{cases} \tag{10}$$

where $\mathbf{x}$ = state vector, $\mathbf{u}$ = plant inputs, $\mathbf{w}$ = exogeneous inputs, $\mathbf{z}$ = control objectives outputs and $\mathbf{y}$ = measured outputs.

The main control requirement of a WECS is to reduce detrimental dynamic loads on shaft, which is obtained from minimizing the shaft torque variations over all bandwidth. In this context, the first control objective output z_1 is obtained weighting the difference $\Delta\omega = \omega_t - \omega_g$ with a fixed gain K_δ. Another important control requirement for fixed and variable speed WECS is the turbine speed control, which can be defined by to reduce speed error $e_t = \omega_{sp} - \omega_t$. Thus, the second control objective output $\mathbf{z_2}$ is generated weighting e_t with a PI function:

$$K_e(s) = \frac{z_2(s)}{e_t(s)} = K_p + \frac{K_i}{s} \tag{11}$$

which implicates in to augment the original nominal model with an integrator. The control design has to minimize the effects of wind fluctuation and ripple torque over the energy delivered to electric load, and the third control objective output $\mathbf{z_3}$ is the generator torque Q_g weighted by a fixed gain K_q. Finally, it is need to limit the bandwitdh of pitch control input β, weighting it by a fixed gain K_β. Admitting $\mathbf{u} = \left[\begin{array}{cc} Q_g & \beta \end{array}\right]'$, $\mathbf{w} = \left[\begin{array}{cc} \omega_{sp} & \dot{V} \end{array}\right]'$ and $\mathbf{x} = \left[\begin{array}{ccccc} Q_a & \omega_t & \omega_g & Q_m & \int e_t dt \end{array}\right]'$, the nominal linearized state model of the pitch regulated WT given by equations

3, 7, 8 and 9, augmented with weighting functions, is described as:

$$\dot{\mathbf{x}} = \left[\begin{array}{cccc|c} \frac{\gamma}{J_t} & -\frac{\gamma(D_t+D_{hg})}{J_t} & \frac{\gamma D_{hg}}{J_t} & -\frac{\gamma}{J_t} & 0 \\ \frac{1}{J_t} & -\frac{D_t+D_{hg}}{J_t} & \frac{D_{hg}}{J_t} & -\frac{1}{J_t} & 0 \\ 0 & \frac{D_{hg}}{J_g} & -\frac{D_{hg}+D_g}{J_g} & \frac{1}{J_g} & 0 \\ 0 & K_{hg} & -K_{hg} & 0 & 0 \\ \hline 0 & -1 & 0 & 0 & 0 \end{array}\right] \mathbf{x} + \left[\begin{array}{cc} 0 & \alpha \\ 0 & 0 \\ 0 & 0 \\ 0 & 0 \\ \hline 1 & 0 \end{array}\right] \mathbf{w} + \left[\begin{array}{cc} 0 & \kappa \\ 0 & 0 \\ -\frac{1}{J_g} & 0 \\ 0 & 0 \\ \hline 0 & 0 \end{array}\right] \mathbf{u} \tag{12}$$

$$\mathbf{z} = \left[\begin{array}{cccc|c} 0 & K_\delta & -K_\delta & 0 & 0 \\ 0 & -K_p & 0 & 0 & K_i \\ 0 & 0 & 0 & 0 & 0 \\ 0 & 0 & 0 & 0 & 0 \end{array}\right] \mathbf{x} + \left[\begin{array}{cc} 0 & 0 \\ K_p & 0 \\ 0 & 0 \\ 0 & 0 \end{array}\right] \mathbf{w} + \left[\begin{array}{cc} 0 & 0 \\ 0 & 0 \\ K_q & 0 \\ 0 & K_\beta \end{array}\right] \mathbf{u} \tag{13}$$

$$\mathbf{y} = \left[\begin{array}{cccc|c} 0 & 0 & -1 & 0 & 0 \end{array}\right] \mathbf{x} + \left[\begin{array}{cc} 1 & 0 \end{array}\right] \mathbf{w} + \left[\begin{array}{cc} 0 & 0 \end{array}\right] \mathbf{u} \tag{14}$$

Table 1. Normalized Parameters: Base value: 2.5 MVA and 1.84 rad/sec

Drive Train Parameters					
$J_t = 37,413$	$D_t = 2,024 \times 10^{-2}$	$J_g = 2,091$	$D_g = 3,01 \times 10^{-2}$	$K_{hg} = 28,4$	D_{hg}=1,831
Linearized Aerodynamical Parameters					
	$\alpha = 7.6949$	$\gamma = -16.1814$	$\kappa = -144.5773$		
Weighting Functions					
	$K_\delta = 5$	$K_q = 1$	$K_\beta = 10$	$K_e(s) = 1.5 + \frac{1}{s}$	

Normalized parameters of a 2.5 MW Horizontal Axis WT connected to four pole generator via a gearbox (Wasynczuk *et al.*, 1981) are presented in the table 1. The frequency response of open-loop WECS is shown in the figure 5. The close-loop WECS is simulated using a non linear model of a WT developed in (Wasynczuk *et al.*, 1981). Although high frequency wind fluctuations are well rejected, WECS is very affected by low frequency wind disturbances. It is noted that control input β is more effective on WT regulation than Q_g, although it reduces the efficiency on energy conversion. Torsional modes can be excited by sudden wind variations and/or operational disturbances since this WECS presents a ressonance peek on:

$$\omega_{res} = \sqrt{K_{hg}\left(\frac{1}{J_t} + \frac{1}{J_g}\right)} = 1.9752 \quad rad/s \tag{15}$$

4. H_2 Controller Design

The H_2 controller design can be formalized as a optimization problem, where the goal is to find a controller $\mathbf{K_2}$ which stabilizes internally the system $\mathbf{G}(s)$ so that H_2 norm:

$$||\mathbf{H_{zw}}||_2 = \sqrt{\frac{1}{2}\int_{-\infty}^{+\infty} [\mathbf{H_{zw}}(j\omega)\mathbf{H_{zw}}^H(-j\omega)]d\omega} \tag{16}$$

is minimized, where $\mathbf{H_{zw}}$ denotes the transfer function matrix from exogeneous inputs $\mathbf{w}$ to objective outputs $\mathbf{z}$. This H_2 optimization problem is equivalent to conventional problem LQG (Skogestad and Postlethwaite, 2001), involving a cost function:

$$J = \int_0^\infty \left[\begin{array}{cc} \mathbf{x}' & \mathbf{u}' \end{array}\right] \left[\begin{array}{cc} \mathbf{C_1'C_1} & \mathbf{C_1'D_{12}} \\ \mathbf{D_{12}'C_1} & \mathbf{D_{12}'D_{12}} \end{array}\right] \left[\begin{array}{c} \mathbf{x} \\ \mathbf{u} \end{array}\right] dt \tag{17}$$

with correlated white noises ξ (states) and η (measurements) entering in the system via $\mathbf{w}$ channel associated with correlation function:

$$E\left\{\left[\begin{array}{cc} \xi(\tau)\xi'(\tau) & \xi(t)\eta'(\tau) \\ \eta(\tau)\xi'(t) & \eta(\tau)\eta'(\tau) \end{array}\right]\right\} = \left[\begin{array}{cc} \mathbf{B_1B_1'} & \mathbf{B_1D_{12}'} \\ \mathbf{D_{12}B_1'} & \mathbf{D_{12}D_{12}'} \end{array}\right]' \delta(t-\tau) \tag{18}$$

This problem can be realizable through of resolution of two Riccatti equations

$$\mathbf{Y_2A'} + \mathbf{AY_2} - \mathbf{Y_2C_2'C_2Y_2} + \mathbf{B_1B_1'} = \mathbf{0} \tag{19}$$

$$\mathbf{A'X_2} + \mathbf{X_2A} - \mathbf{X_2B_2B_2'X_2} + \mathbf{C_1C_1'} = \mathbf{0} \tag{20}$$

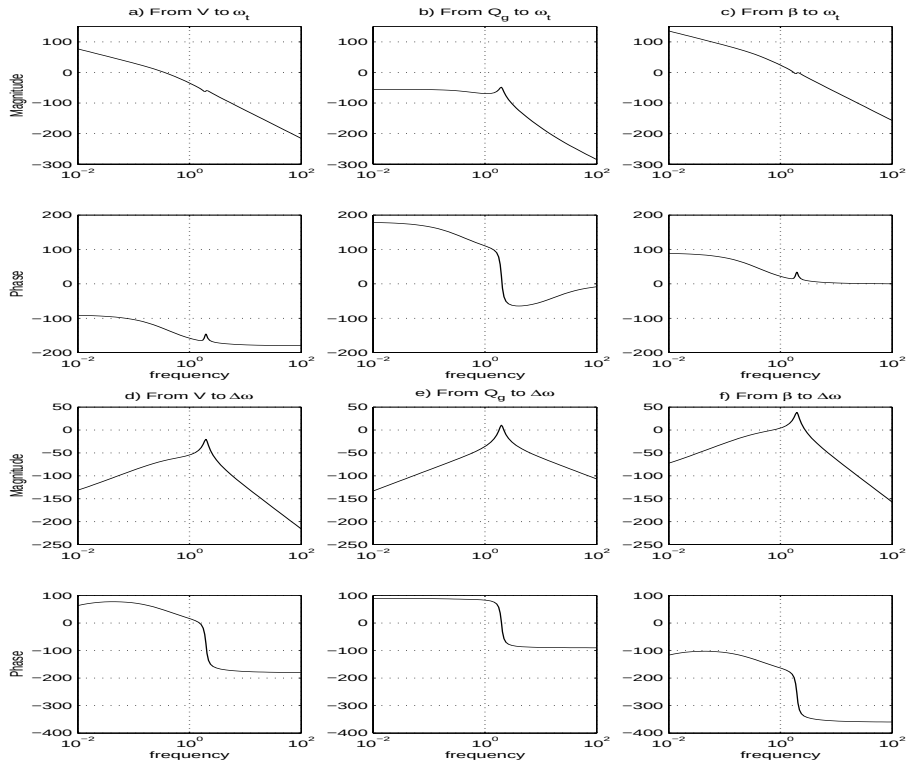

Figure 5. Bode plots of linearized open-loop WECS model

resulting in H_2 optimal controller $K_2(s)$ given by:

$$\mathbf{K_2}(s) = \begin{cases} \dot{\hat{\mathbf{x}}} = (\mathbf{A} - \mathbf{B_2}\mathbf{B_2'}\mathbf{X_2} - \mathbf{Y_2}\mathbf{C_2'}\mathbf{C_2})\,\hat{\mathbf{x}} + \mathbf{Y_2}\mathbf{C_2'}\mathbf{y} \\ \mathbf{u} = -\mathbf{B_2'}\mathbf{X_2}\hat{\mathbf{x}} \end{cases} \tag{21}$$

Considering the WECS model developed in section 2. and the weighting functions presented in the table 1, this design procedure results in the following H_2 controller:

$$\mathbf{K}_2(s) = \begin{bmatrix} \frac{0.07592s^4 - 0.6462s^3 - 3.923s^2 - 2.761s - 0.7238}{(s^5 + 4.504s^4 + 11.09s^3 + 13.27s^2 + 7.454s + 7.547\times10^{-6}} \\ \frac{-0.2345s^4 - 0.6949s^3 - 1.269s^2 - 0.5969s - 0.07599}{s^5 + 4.504s^4 + 11.09s^3 + 13.27s^2 + 7.454s + 7.547\times10^{-6}} \end{bmatrix}$$

The frequency response of closed-loop WECS with H_2 controller is shown in the figure 6. High frequency wind fluctuations are submitted to a strong attenuation. For frequencies below 0.7 rad/s, sensitivity function, given by transfer function e_t/ω_{sp}, decays rapidly when the frequency tends to zero, as shown its Bode plots, satisfying requirements related to disturbance rejections. The Bode plots for complementary sensitivity function, given by transfer function ω_g/ω_{sp}, shows that H_2 controller attenuates measurements noise above 0.7 rad/s, assuring good robustness against uncertainties above of this frequency. Considering speed difference $\Delta\omega$, the excitation of torsional modes is difficult since H_2 control system provides an adequate attenuation for reference variations and/or operational disturbances. Although power fluctuations on electric load are attenuated, system response to variations on electric torque Q_g, one of control input, will be very slow.

The fixed-speed operation of closed-loop WECS with H_2 controller is shown in the figure 7. Aiming to verify the dynamical behaviour of the control system, this WECS is submitted to wind gust with duration of 90 s. After this event, it is need approximately 5 minutes for ω_t returns to its reference value ω_{sp}, where both control inputs are simultaneously used on speed regulation. Considering fixed-speed operation, this control system presented a unstable behavior for greatest disturbances. Admitting variable speed operation, simulation results of dynamic behavior of closed-loop WECS with H_2 controller submitted to wind step variation of 7.5 m/s to 9.5m/s are shown in the figure 8. In this case, the speed reference is adjusted to:

$$\omega_{sp} = \frac{\lambda_{opt}}{R} V \tag{22}$$

With the ocurrence of wind step, ω_t follows speed reference ω_{sp}, reaching zero error after 10 minutes. Aiming to adjust ω_t, generator torque Q_g is practically duplicated, increasing the energy delivered to electric load. Considering that β has a detrimental effect on energy conversion efficiency, the relatively small contribution of this control input on speed regulation is positive to variable speed WECS. The system operation does not excite any torsional modes and the noises introduced by wind fluctuation are filtered by H_2 controller.

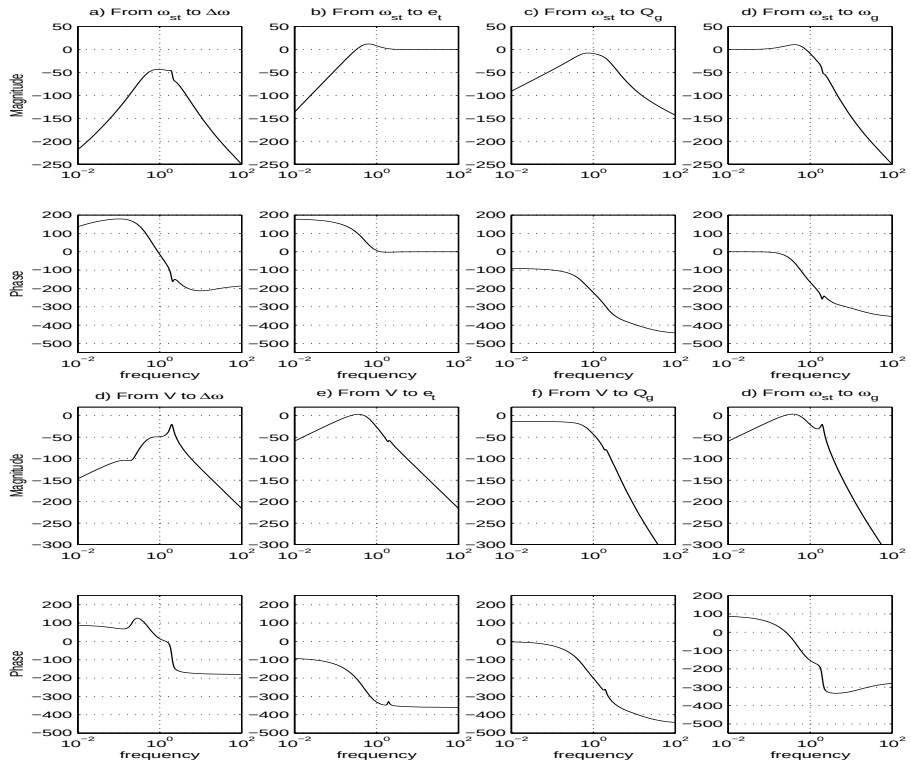

Figure 6. Bode plots of close-loop WECS with H_2 controller

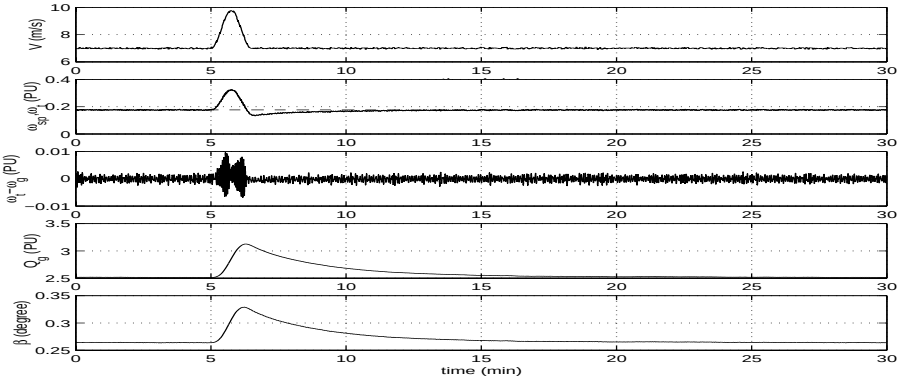

Figure 7: Normalized dynamical behavior of close-loop WECS with H_2 controller from wind gust considering fixed-speed operation

5. H_∞ Controller Design

Feedback control design can be also formalized in terms of H_∞ norm optimization. The sub-optimal H_∞ control problem is to find all admissible compensator $\mathbf{K}_\infty(\mathbf{s})$ which stabilizes internally the generalized system $\mathbf{G}(\mathbf{s})$ and minimizes the norm (Doyle *et al.*, 1989):

$$||\mathbf{H_{zw}}||_\infty = \sup_\omega \bar{\sigma}[\mathbf{H_{zw}}] \tag{23}$$

such that $||\mathbf{H_{zw}}||_\infty < \epsilon$. Considering $\mathbf{D_{11}} = \mathbf{0}$ and $\mathbf{D_{22}} = \mathbf{0}$, the solution of this problem can be given by:

$$\mathbf{K}_\infty(s) = \begin{cases} \dot{\hat{\mathbf{x}}} = (\mathbf{A}_\infty - \mathbf{B_2}\mathbf{B_2'}\mathbf{X}_\infty - \mathbf{L}_\infty\mathbf{C_2})\,\hat{\mathbf{x}} + \mathbf{L}_\infty\mathbf{y} \\ \mathbf{u} = -\mathbf{B_2'}\mathbf{X}_\infty\hat{\mathbf{x}} \end{cases} \tag{24}$$

where

$$\mathbf{A}_\infty = \mathbf{A} + \epsilon^{-\mathbf{2}}\mathbf{B_1}\mathbf{B_1'}\mathbf{X}_\infty \tag{25}$$

$$\mathbf{L}_\infty = \left(\mathbf{I} - \epsilon^{-\mathbf{2}}\mathbf{Y}_\infty\mathbf{X}_\infty\right)^{-\mathbf{1}}\mathbf{Y}_\infty\mathbf{C_2'} \tag{26}$$

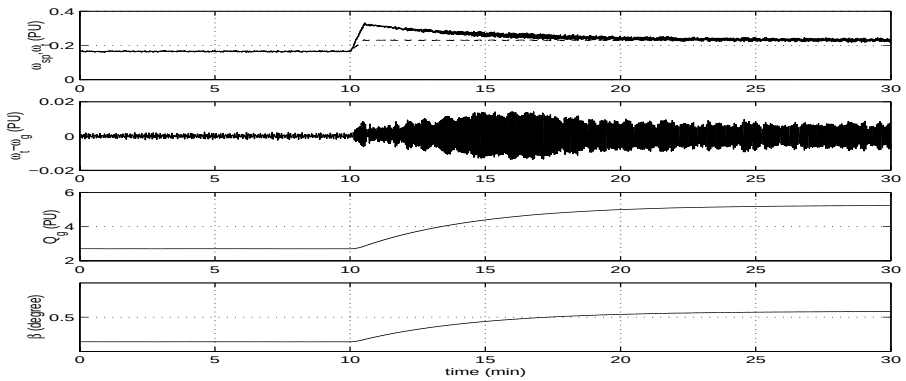

Figure 8: Normalized dynamical behavior of close-loop WECS with H_2 controller from wind step considering variable-speed operation

and $\mathbf{X}_\infty$ and $\mathbf{Y}_\infty$ are the solutions of two Riccatti equations:

$$\mathbf{A}'\mathbf{X}_\infty + \mathbf{X}_\infty\mathbf{A} - \mathbf{X}_\infty\mathbf{B}_\infty\mathbf{B}'_\infty\mathbf{X}_\infty + \mathbf{C}'_1\mathbf{C}_1 = \mathbf{0} \tag{27}$$

$$\mathbf{Y}_\infty\mathbf{A} + \mathbf{A}'\mathbf{Y}_\infty - \mathbf{Y}_\infty\mathbf{C}'_\infty\mathbf{C}_\infty\mathbf{Y}_\infty + \mathbf{B}_1\mathbf{B}'_1 = \mathbf{0} \tag{28}$$

where

$$\mathbf{B}_\infty\mathbf{B}'_\infty = \epsilon^{-2}\mathbf{B}_1\mathbf{B}'_1 - \mathbf{B}_2\mathbf{B}'_2 \tag{29}$$

$$\mathbf{C}_\infty\mathbf{C}'_\infty = \epsilon^{-2}\mathbf{C}_1\mathbf{B}'_1 - \mathbf{C}_2\mathbf{C}'_2 \tag{30}$$

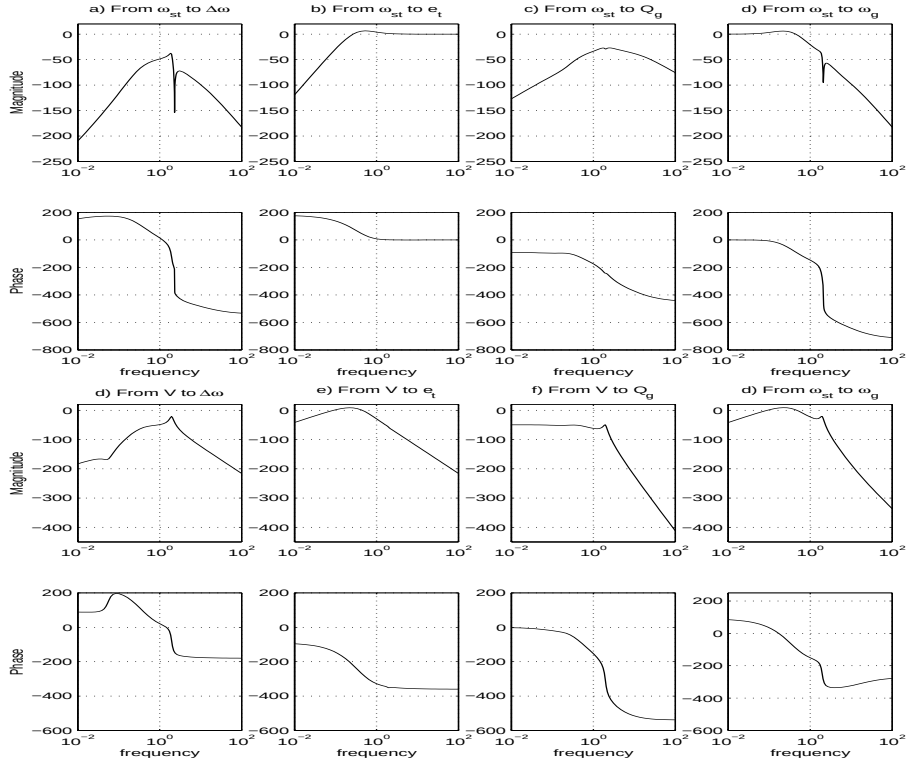

Figure 9. Bode plots of close-loop with H_∞ controller

The conditions to assure the existence of a solution for H_∞ control problem are $\mathbf{X}_\infty \geq \mathbf{0}$, $\mathbf{Y}_\infty \geq \mathbf{0}$ and the eigenvalues $\rho(\mathbf{X}_\infty\mathbf{Y}_\infty) \leq \epsilon^2$. The best solution for sub-optimal optimal H_∞ controller can be computed using the loop-shifting two-Riccatti formulae (Chang and Safonov, 1996). Considering the WECS model developed in section 2. and the weighting functions presented in the table 1, the optimal H_∞ controller for WECS, obtained with $\epsilon = 0.0674$,

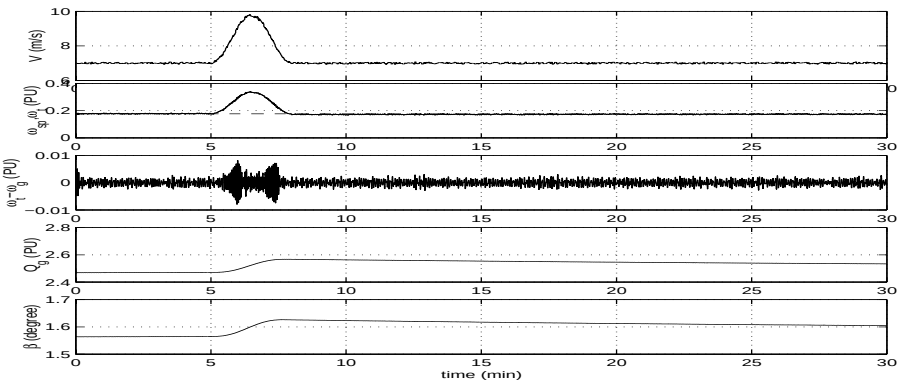

Figure 10: Normalized dynamical behavior of close-loop WECS with H_∞ controller from wind gust considering fixed-speed operation

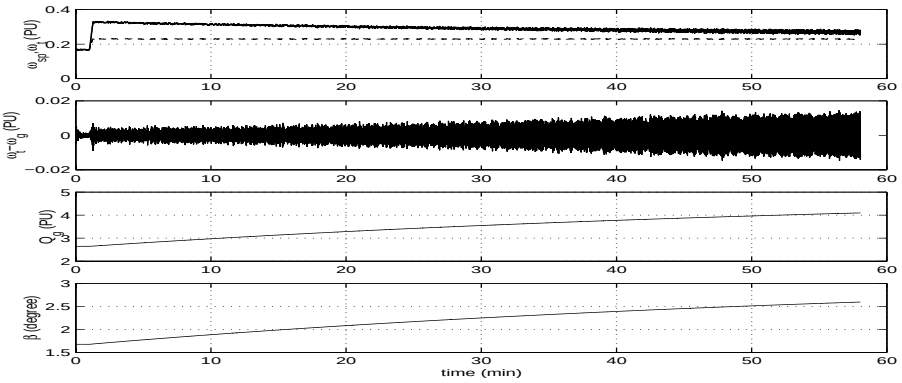

Figure 11: Normalized dynamical behavior of close-loop WECS with H_∞ controller from wind step considering variable-speed operation

is given by:

$$\mathbf{K}_\infty(s) = \begin{bmatrix} \frac{2.297s^4-2.253s^3-8.93s^2-2.685s-0.3474}{s^5+16.25s^4+52.89s^3+92.42s^2+51.75s+5.18\times10^{-5}} \\ \frac{-1.138s^4-3.18s^3-6.059s^2-2.58s-0.22}{s^5+16.25s^4+52.89s^3+92.42s^2+51.75s+5.18\times10^{-5}} \end{bmatrix}$$

The frequency response of closed-loop WECS with H_∞ controller is shown in the figure 9, where is noted that high frequency wind fluctuations are strongly attenuated. Below 0.7 rad/s, sensitivity function decays rapidly while above this frequency complementary sensitivity function is attenuated, which assures requirements related to disturbance rejections and robustness against uncertainties. Such as H_2, H_∞ control system provides an adequate attenuation for reference variations and/or operational disturbances. If compared to H_2, H_∞ controller provides a greatest attenuation for power fluctuations on electric load are attenuated, which become its response extremely slow for variations on electric torque Q_g.

The figure 10 shows a fixed-speed operation of closed-loop WECS with H_∞ controller when submitted to wind gust with duration of 180 s. If compared with H_2 controller, control systems designed using H_∞ philosophy have a better robustness, without to present a unstable behavior when submitted to greatest disturbances. Using β and Q_g, the control system is able to reject the effects of this wind disturbance, and ω_t returns to its reference value ω_{sp} approximately after the end of the wind gust. Admitting variable speed operation, simulation results of dynamic behavior of closed-loop WECS with H_∞ controller submitted to wind step variation of 7.5 m/s to 9.5m/s are shown in the figure 11. It is noted that β performance on speed adjust is improved. Although ω_t will reach the reference ω_{sp}, this adjust is extremely slow.

6. Conclusion

Although H_2 and H_∞ approximations used in controller designs present several similarities, the H_∞ design results in a more conservative controller, since H_∞ philosophy includes dependency of the disturbance signal. In this context, the H_∞ design will present better robustness than a similar H_2 design. However, this property has a cost and implicates in slowest dynamic response in close-loop WECS with H_∞ controllers. Thus, the performance of close-loop WECS with H_∞ controllers will be better in regulation applications, such as fixed speed operations or cases where the wind speed presents a behaviour without dramatic variations. In counterparts, variable speed WECS consists in

a tracking problem, where the main objective is to follow a reference imposed by wind speed. In this case, a fast response is important and the performance of the H_2 controller is better if compared to H_∞ controller. Although H_∞ solution is relatively flexible admitting sub-optimal controllers, the tendency observed in this work is that H_∞ controller is more adequate for fixed-speed close-loop WECS while H_2 controller is more adequate for variable-speed close-loop WECS.

References

Chang, R. Y. and Safonov, M. G., 1996, "*Robust control toolbox for use with matlab* ", Mathworks Inc. USA.

Dessaint, L., Nakra, H. and Mukhedkar, D., 1986, " Propagation and elimination of torque ripple in a wind energy conversion system", *IEEE Trans. on Energy Conversion* , Vol. **1**, No. 2 , pp. 104–112.

Doyle, J. C., Glover, K., Khargonekar, P. P. and Francis, B. A., 1989, " State-space solutions to standart H_2 and H_∞ control problems", *IEEE Trans. on Automatic Control* , Vol. **34**, No. 8 , pp. 831–846.

Freris, L. L., Ed.), 1990, "*Wind Energy Conversion Systems* ", Prentice Hall Inc. United King.

Lefevbre, S. and Dubé, B., 1988, " Control system analysis and design for an aerogenerator with eigenvalue methods", *IEEE Trans. on Power Systems* , Vol. **3**, No. 4 , pp. 1600–1608.

Leith, D. J. and Leithead, W., 1997, " Implementation of wind turbine controllers", *International Journal of Control* , Vol. **66**, No. 3 , pp. 349–380.

Leithead, W. E., de la Salle, S. and Reardon, D., 1991, " Role and objectives of control for wind turbines", *IEE proceedings-C* , Vol. **138**, No. 2 , pp. 135–148.

Maciejowski, J. M., 1989, "*Multivariable Feedback Design* ", Addison-Wesley Publishing Company Inc. Wokingham - England.

Manwell, J. F., McGowan, J. G. and Bailey, B. H., 1991, " Electrical / mechanical options for variable speed wind turbines", *Solar Energy* , Vol. **46**, No. 1 , pp. 41–51.

Novak, P., Ekelund, T., Jovik, I. and Schmidtbauer, B., 1995, " Modeling and control of variable-speed wind-turbine drive-system dynamics", *IEEE Control Systems* , Vol. **15**, No. 4 , pp. 28–38.

Rocha, R. and Martins Filho, L. S., 2003, " A multivariable H_∞ control for wind energy conversion system", *IEEE Conference on Control Applications* IEEE Istambul - Turkey.

Skogestad, A. and Postlethwaite, I., 2001, "*Multivariable Feedback Control - Analysis and Design* ", 2.a ed. John Wiley and Sons.

Wasynczuk, O., Man, D. T. and Sullivan, J. P., 1981, " Dynamic behaviour of a class of wind turbine generators during random wind fluctuatons", *IEEE Trans. on Power Apparatus and Systems* , Vol. **100**, No. 6 , pp. 2837–2845.

7. Responsibility notice

The authors are the only responsible for the printed material included in this paper.